Preprints, 25th International Conf. on Radar Meteorology. AMS, Paris, FRANCE, June 24-28, 1991, 131-134.

5.1

APPLICATION OF A THERMODYNAMIC RETRIEVAL TECHNIQUE TO A NUMERICAL MODEL

Ju Sun and R.A. Houze, Jr.

Department of Atmospheric Sciences
University of Washington
Seattle, WA 98195 USA

1. INTRODUCTION

Doppler-radar observational technology provides the opportunity to study convective cloud systems by indicating the detailed air circulation inside of them. In addition, it is possible to retrieve thermodynamic parameters from the indicated wind field. Gal-Chen (1978) and Hane and Scott (1978) initiated thermodynamic retrieval work by proposing an analysis based on the equation of motion. Roux (1985, 1988) attempted to improve this technique by using the equation of motion in conjunction with the thermodynamic equation. Further improvement of the retrieval is described in Roux and Sun (1990, henceforth RS). Although their application of this technique to a west African squall line observed during the COPT81* experiment produced physically reasonable results, a strict validation of the retrieval technique was not conducted. We have used the output of the two-dimensional model of Fovell and Ogura (1988) to test the retrieval method described in RS. Their model simulates a midlatitude squall line similar to the west African squall line to which RS's retrieval was applied. Our main objectives are to determine: (i) whether there is a limitation of the computational technique involved in the retrieval; (ii) whether the mean thermodynamic structure can be determined from the time-mean winds, such as those available from a time-space composite of radar data; and (iii) what time resolution is required to obtain accurate retrievals of the thermodynamic structure at an instant of time, i.e. what maximum time between radar scans can be expected to give reliable retrieval results.

2. DESCRIPTION OF RETRIEVAL TECHNIQUE AND MODEL OUTPUT

The basic premise of the retrieval is that unknown thermodynamic parameters like temperature and pressure can be deduced from observed wind velocities. These variables are related to each other through the anelastic form of the basic governing equations of the atmosphere (e.g. by Wilhelmson and Ogura 1972). These include the equation of motion

$$\frac{\partial \vec{v}}{\partial t} + (\vec{v}\cdot\nabla)\vec{v} = -c_p\,\theta_{v0}\nabla\pi_1 + g\left(\frac{\theta_{c1}}{\theta_0} - q_r\right)\vec{k} + \vec{F}_{tur} \quad (1)$$

and the thermodynamic equation

$$\frac{\partial}{\partial t}(\theta_0 + \theta_1) + (\vec{v}\cdot\nabla)(\theta_0 + \theta_1) = S_\theta\,, \quad (2)$$

where $\vec{v}$ is the wind velocity, c_p is the specific heat at constant pressure, θ_{v0} is the virtual potential temperature of the base state (environment), θ_0 is the base-state potential temperature, π_1 is the non-dimensional pressure perturbation, g is the gravitational acceleration, θ_{c1} is the cloud-virtual temperature perturbation, q_r is the precipitation mixing ratio, $\vec{k}$ is the unit vector in the vertical, $\vec{F}_{tur}$ is the turbulence force, and t is time. Details are given by RS. We find the θ_{c1} and π_1 fields by minimizing the integrals

$$F_\theta = \iint \left(\frac{\partial\theta_{c1}}{\partial x} - B_x\right)^2 + \mu_0 f(V)\left(\frac{u}{V}\frac{\partial\theta_{c1}}{\partial x} + \frac{w}{V}\frac{\partial\theta_{c1}}{\partial z} - B_t\right)^2 + \mu_1 h(V,w)\left(\frac{\partial\theta_{c1}}{\partial z}\right)^2 dx\,dz, \quad (3)$$

$$F_\pi \equiv \iint\left[\left(\frac{\partial\pi_1}{\partial x} - A_x\right)^2 + \left(\frac{\partial\pi_1}{\partial z} - A_z\right)^2\right] dx\,dz\,, \quad (4)$$

where x is the horizontal coordinate, z is the vertical coordinate, $A_x \equiv \partial\pi_1/\partial x$, $A_z \equiv \partial\pi_1/\partial z$, $B_x \equiv \partial\theta_{c1}/\partial x$, $B_t \equiv u\partial\theta_{c1}/\partial x + w\partial\theta_{c1}/\partial z$, $V \equiv \sqrt{u^2+w^2}$, μ_0 and μ_1 are adjustable constants, and $f(V)$ and $h(v,w)$ are special weighting functions defined in RS. A_x, A_z, B_x, and B_t are considered known from observations. Expressions for these terms are obtained from the remaining terms in (1) and (2). Radar-observed winds and reflectivity are substituted into these expressions. See RS for details. The values of A_x, A_z, B_x, and B_t determined from observations are substituted in (3) and (4) and integrations are carried out over the whole domain. When the terms on the left-hand side of (1) are estimated from real Doppler-radar data, it is often difficult or impossible to estimate the local derivatives $\partial u/\partial t$ and $\partial w/\partial t$. It may be necessary in practice to avoid these terms by seeking relatively steady-state features in the data or by applying the technique to mean or composite wind fields. If the latter is done (e.g. Sun and Roux 1988; Roux and Sun 1990) an error is introduced because the average of the terms $(\vec{v}\cdot\nabla)w$ and $(\vec{v}\cdot\nabla)u$ are estimated from the mean velocity fields as $(\bar{\vec{v}}\cdot\nabla)\bar{w}$ and $(\bar{\vec{v}}\cdot\nabla)\bar{u}$, where the overbars represent time averages. This estimate ignores the contributions of eddy fluxes $\overline{(\vec{v}'\cdot\nabla)w'}$ and $\overline{(\vec{v}'\cdot\nabla)u'}$, where the prime represents a deviation from the time average. One of the main objectives of this paper is to evaluate how much impact the neglect of the eddy flux term has on the retrieval of thermodynamic fields of the squall line with a trailing-stratiform region. We can make this determination with the model results used as input.

Fovell and Ogura's (1988) simulation was carried out with an anelastic two-dimensional model, in which the

* *CO*nvection *P*rofonde *T*ropicale 1981.

Coriolis force is neglected and the turbulence term is set to a very small value. It produced a moving squall line with periodic formation of convective cells at the leading edge of the storm. The individual cells moved rearward and each complete cycle lasted about 32 min. The time-averaged fields over one or several complete cycles have the principal characteristics of observed squall lines (Fig. 1). Below a layer of front-to-rear flow, a rear inflow enters the system between the 1- and 3-km levels. The strongest vertical motions are found in the leading portion of the storm (right-hand side of figure panels). A deep downdraft originating at the top of the storm is located just behind the zone of upward motion. Farther toward the rear, weaker but broader updraft and downdraft are separated at the 6-km level. The cloud-virtual potential temperature perturbations (θ_{cl}) are positive at upper levels. At the front, the warm air extends through a very narrow zone. The negative perturbations at lower levels form the "cold pool."

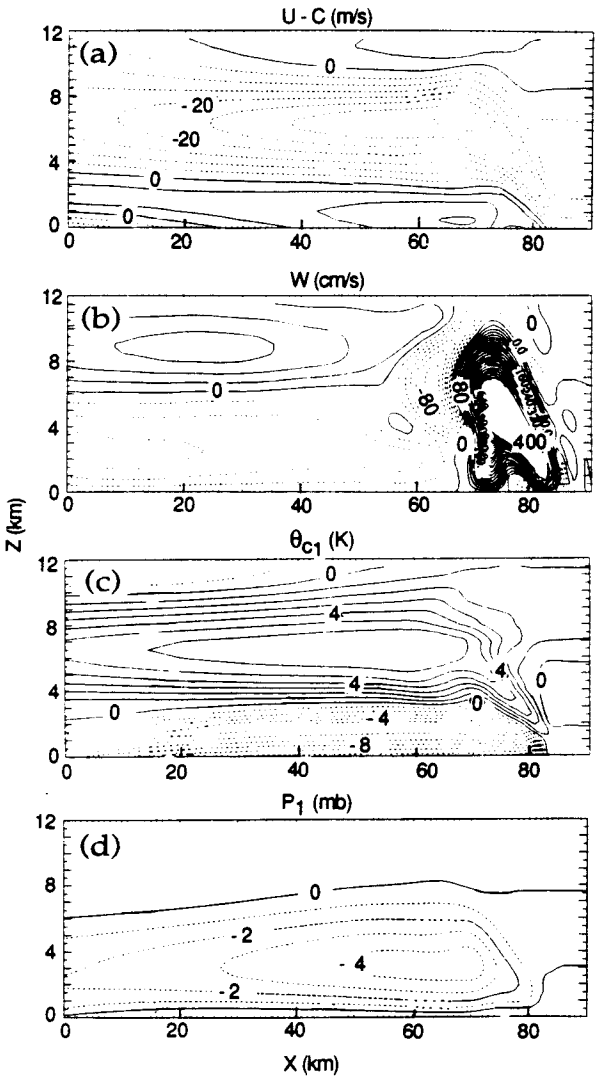

Fig. 1 Time-averaged model fields. (a) System-relative horizontal velocity (5 m s^{-1}); (b) Vertical velocity (20 cm s^{-1}); (c) Virtual cloud potential temperature perturbation (1°K); (d) Pressure perturbation (1 mb).

3. RETRIEVAL BASED ON THE TIME-AVERAGED MODEL WIND FIELDS

The first objective of this study listed in the introduction may be restated as the question: Can we find the θ_{cl} field without any purely computational flaw if the terms B_x and B_t are deduced correctly? The second objective may be rephrased as: Is it possible to estimate the terms B_x and B_t correctly from the steady time-mean winds? We now address the first question to make sure there is no distortion associated with the computational technique before we attempt to address the second objective.

Our present concern is whether we can determine the θ_{cl} field correctly, given accurate values of B_x and B_t. The "correct" values of B_x and B_t are calculated from the model output θ_{cl}. These values, called B_{xm} and B_{tm}, are computed by finite differences substituted into (3). After some trials, the best retrieved θ_{cl} field is obtained when the constants involved in Eq. (3) are set in the following combination: V_0=4 m s^{-1}, μ_0= 0.2, μ_l=0. Comparison of the retrieved θ_{cl} field with the simulation output (not shown here) is very good. A similar effort is made to retrieve the pressure perturbation field p_l. The retrieved p_l field is nearly identical to the simulation output. Thus, if we can estimate B_x and B_t correctly from the observed wind field, there is virtually no obstacle to correctly retrieving the temperature perturbation θ_{cl} field.

The problem becomes how to estimate the B_x and B_t in an appropriate way, which is our second objective. To simulate a composite of radar data, we consider the case in which the model wind and reflectivity fields are time averaged. In this case, the local time-derivative terms in (1) and (2) vanish. Fig. 2 shows the retrieved temperature and pressure fields. Except for the more irregular shapes of the contours in comparison to the simulation output (Figs. 1c,d), the overall features are evident. Positive θ_{cl} perturbations are found at upper levels with a maximum of 5°C. The upper-level warm air also extends downward at the front of the system. The negative values below indicate the cold pool formed by the evaporation of precipitation. The pressure perturbations, whose vertical structures are mainly determined by the temperature perturbations through the hydrostatic effect, show a low of -3 mb at the 3.5-km level.

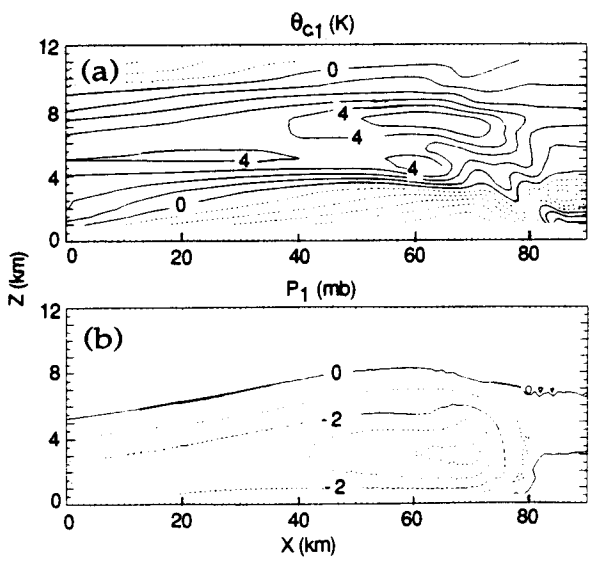

Fig. 2 (a) Retrieved θ_{cl} field with precipitation content q_r deduced from model reflectivity by the relationship $q_r \sim Z$ used by RS; (b) Retrieved p_l field.

The main discrepancies in the retrieved temperature and pressure are believed to be the consequence of ignoring the eddy flux terms $\overline{(\vec{v}'\cdot\nabla)w'}$ and $\overline{(\vec{v}'\cdot\nabla)u'}$ in the expression for B_x. This conclusion is supported by a retrieval experiment in which the B_x field computed from the velocity fields is replaced by the accurate value B_{xm} deduced from the simulation output θ_{cl} field. The favorable comparison of the model and retrieved fields in Figs. 1c and 2a throughout the stratiform region suggests that retrievals applied to mean or composite radar data fields will be more accurate in the stratiform region than in the highly convective region of the leading line, where the eddy fluxes are probably strong.

4. RETRIEVAL BASED ON THE MODEL INSTANTANEOUS FIELDS

We have now seen that reasonably accurate results may be expected if the retrieval is applied to the time-mean wind fields of the stratiform region of a squall line with a trailing-stratiform region; however, the highly fluctuating wind fields in the convective region lead to errors in the retrieval applied to the mean winds in that zone. In the absence of some parameterization of the missing eddy flux terms, it is necessary to apply the retrieval to the instantaneous wind field in the convective region in order to infer the thermodynamic structure of the convective zone. In this subsection, we explore the accuracy of the retrieval when applied to the instantaneous fields. In particular, we investigate the time resolution required to obtain accurate results.

The instantaneous model fields at 576 min are for a time slightly before the main cell reached its maximum rainfall intensity. Verification of the computational step again shows that the basic computational technique is valid.

To measure the total impact of the local change of the wind field, the retrieval was first made without local time derivatives. Although we have positive perturbations at upper levels and negative ones below, the original θ_{cl} field is not distinguishable. This result indicates that the evolution of the simulated squall line is too important to be neglected. Since the simulated squall line does not always evolve linearly, the local time derivatives vary in value as the size of the time interval centered at a particular time varies. Table 1 indicates the accumulated errors E_x and E_t, defined as

$$E_x = \frac{\iint (B_x - B_{xm})^2\,dx\,dz}{\iint (B_{xm})^2\,dx\,dz}\ ,\ E_t = \frac{\iint (B_t - B_{tm})^2\,dx\,dz}{\iint (B_{tm})^2\,dx\,dz}\ ,$$

where B_x and B_t are calculated with different intervals. When the local time derivatives are taken into account, both B_x and B_t are greatly improved. However, the error for calculations centered at 576 min is not very sensitive to the size of the time interval since the tendency around this time

Table 1 Deviations of B_x and B_t from B_{xm} and B_{tm} at 576 min with and without taking into account the local time derivatives.

time interval	E_x	E_t
No	2.49	1.22
± 2 min	0.76	0.52
± 1 min	0.55	0.48
± 15 s	0.50	0.52

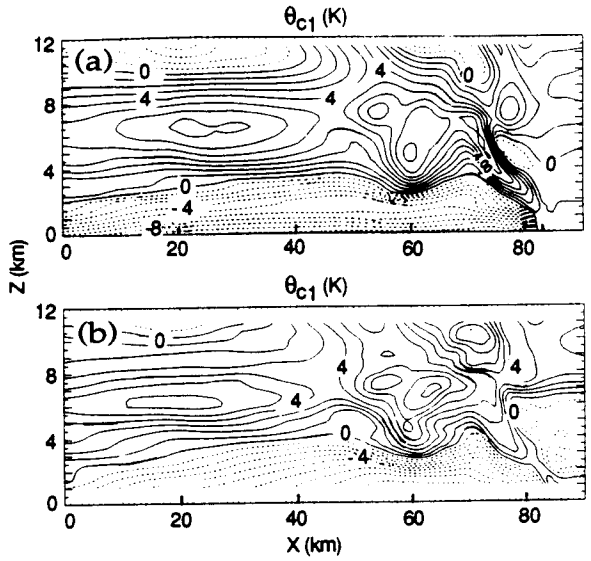

Fig. 3 Instantaneous model field at 576 min. (a) Virtual cloud potential temperature perturbation (1°K). (b) Retrieved θ_{cl} field with local time derivatives calculated from ±1 min interval.

Table 2. As in Table 1, except at 566 min.

time interval	E_x	E_t
No	7.80	1.38
± 2 min	4.24	0.62
± 1 min	2.18	0.44
± 15 s	1.33	0.41

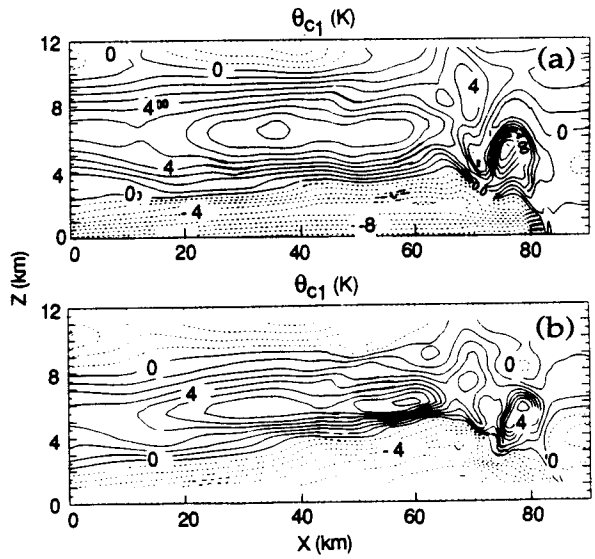

Fig. 4 Instantaneous wind field at 566 min. (a) Virtual cloud potential temperature perturbation (1°K). (b) Retrieved θ_{cl} field with local time derivatives calculated from ±15 s interval.

is quite linear. For purposes of illustration, we choose the ±1 min interval. The retrieval results are shown in Fig. 3b. We find virtually all of the features that appear in the model output θ_{cl} field (Fig. 3a). To get a more complete view of the impact of the temporal evolution, we carry out the retrieval at another moment. In contrast to 576 min, the second retrieval at 566 min is situated just after a secondary

rainfall maximum where the tendency is strongly decreasing. Table 2 demonstrates clearly the effect of the deviation of B_x and B_t from B_{xm} and B_{tm} when different intervals centered at 566 min are used. The inclusion of local time derivatives improves the estimation of B_x; however, B_x at 566 min with a ±15 s interval is still high: 1.3 vs. 0.5 at 576 min. This reflects that the temporal changes around 566 min are more important and less linear than at 576 min. When the interval is fixed at ± 15 s, the retrieval with the moist adiabat of 16°C gives the temperature perturbations shown in Fig. 4b. Compared with the model output θ_{cl} field (Fig. 4a), the main features are evident. At time intervals of ±1 min and greater, most of the features of the model simulation are still present in a qualitative sense, but are grossly exaggerated quantitatively.

5. CONCLUSIONS

A thermodynamic retrieval technique, based on the equation of motion and thermodynamic equation and previously applied to a west African squall line with trailing-stratiform precipitation, has been validated by applying it to a two-dimensional numerical model simulation of a similar squall-line cloud system. Model wind and reflectivity output are used as input to the retrieval, and the model thermodynamic output provides a check on the performance of the retrieval. The computational technique is found to be valid by these comparisons. Application of the retrieval to the time-averaged fields showed that the neglect of eddy correlation terms in the retrieval introduces errors in the retrieval results which can be quite large in convective regions but are not serious in the stratiform zone. When applied to instantaneous model output fields, it is found that serious errors may occur in the retrieval when local time changes are large and nonlinear. If the time resolution is not ≤ about 2 min, one cannot be confident in the retrieval.

ACKNOWLEDGMENTS

The main software used in this study was developed originally by Dr. Frank Roux at Centre de Recherches en Physiques de l'Environnement Terrestre et Planetaire (CRPE / CNET-CNRS) in Issy-Les-Moulineaux, France. Model output was provided by Dr. R.G. Fovell, G.C. Gudmundson edited the manuscript, and K. Dewar drafted the figures. This research was sponsored by National Science Foundation grant ATM-8719838.

REFERENCES

Fovell, R.G., and Y. Ogura, 1988: Numerical simulation of a midlatitude squall line in two dimensions. *J. Atmos. Sci.*, **45**, 3846-3879.

Gal-Chen, T., 1978: A method for the initialization of the anelastic equation: Implication for matching models with the observations. *Mon. Wea. Rev.*, **106**, 587-606.

Hane, C.E., and B.C. Scott, 1978: Temperature and pressure perturbations within convective clouds derived from detailed air motions: Preliminary testings. *Mon. Wea. Rev.*, **106**, 651-661.

Roux, F., 1985: Retrieval of thermodynamic fields from multi-Doppler radar data using the equations of motion and the thermodynamic equation. *Mon. Wea. Rev.*, **113**, 2142-2157.

Roux, F., 1988: The west African squall line observed on 23 June 1981 during COPT81: Kinematics and thermodynamics of the convective region. *J. Atmos. Sci.*, **45**, 406-426.

Roux, F., and J. Sun, 1990: Single Doppler observations of a west African squall line on 27-28 May 1981 during COPT81: Kinematics, thermodynamics, and water budget. *Mon. Wea. Rev.*, **118**, 1826-1854.

Sun, J., and F. Roux, 1988: Thermodynamic structure of the trailing-stratiform regions of two west African squall lines. *Ann. Geophys.*, **6**, 659-670.

Wilhelmson, R.E., and Y. Ogura, 1972: The pressure perturbation and the numerical modeling of a cloud. *J. Atmos. Sci.*, **29**, 1295-1307.